JOURNAL OF combinatorial CHEMISTRY

Article

Imaging Reflection IR Spectroscopy as a Tool to Achieve Higher Integration for High-Throughput Experimentation in Catalysis Research

Petr Kubanek, Oliver Busch, Stuart Thomson, Hans W. Schmidt, and Ferdi Schth

J. Comb. Chem., **2004**, 6 (3), 420-425• DOI: 10.1021/cc049957e • Publication Date (Web): 30 March 2004

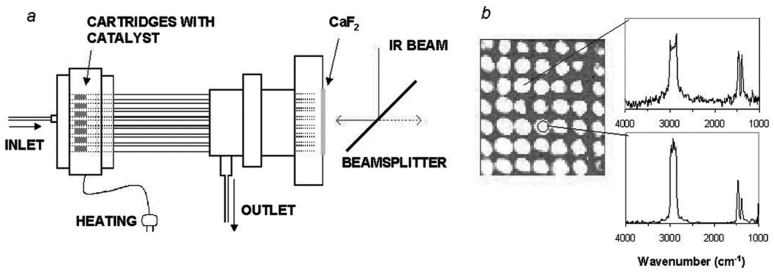

More About This Article

Additional resources and features associated with this article are available within the HTML version:

- Supporting Information
- Access to high resolution figures
- Links to articles and content related to this article
- Copyright permission to reproduce figures and/or text from this article

View the Full Text HTML

Journal of Combinatorial Chemistry is published by the American Chemical Society.
1155 Sixteenth Street N.W., Washington, DC 20036

Imaging Reflection IR Spectroscopy as a Tool to Achieve Higher Integration for High-Throughput Experimentation in Catalysis Research

Petr Kubanek, Oliver Busch, Stuart Thomson, Hans W. Schmidt, and Ferdi Schüth*

Max-Planck Institut für Kohlenforschung, Kaiser Wilhelm Platz 1, 45470 Mülheim, Germany

Received February 16, 2004

FTIR spectroscopy in reflection mode combined with a focal plane array (FPA) detector was employed for high-throughput screening of activity of catalysts in *n*-pentane hydroisomerization. The reactor system was evaluated using reference catalysts Pt-MOR and γ-alumina of known catalytic activity. By using the reflection setup, a higher degree of parallelization was possible, as compared to previous reports, in which transmission cells had been used. The 49-channel parallel reactor in combination with the FPA-IR optical setup was able to provide reliable information about the activity of different catalysts with relative data error of less than ±20%.

Introduction

In the search for new catalysts, systematic exploration of the parameters that control the properties of the catalytic material is necessary. This process can be time-consuming, and thus, over the past years, approaches for parallel or fast serial evaluation of large catalyst libraries have been developed. The main goal of those high-throughput approaches is to obtain the desired information in a relatively short period of time and to decrease the total time required for the development of new catalysts.

Although early attempts to use parallel reactors with common analysis for catalysis studies have been published,[1,2] real breakthroughs in high-throughput experimentation (HTE) in catalysis were achieved only at the end of the 1990s.[3−12] In general, the HTE approach can be used in the discovery mode, where parallelization is massive but the depth of information rather low, or in the optimization mode, where throughput is lower but the data obtained have quality comparable to the data resulting form conventional experiments. In the first case, the type of analysis used often determines the format of the whole test,[4,13−15] whereas for optimization, reactors have been developed which allow the determination of catalyst activity under close-to-conventional conditions.[8,16−18]

It is possible to apply a wide range of different analytical methods for the analysis of the catalyst performance, some of which are fast sequential techniques and some are truly parallelized. Catalyst activity/selectivity can be monitored by simple and easy-to-use techniques in fast sequential mode, such as mass spectrometry,[7,14,19−20] gas chromatography,[18] or infrared spectroscopy[9,21−26] (also truly parallel with FPA detection, as pioneered by the group of Lauterbach[21,24,26]). Parallelized analysis is possible by IR thermography,[3,5,27−28] REMPI (resonance-enhanced multiphoton ionization),[4] photoacoustic detection,[29,30] or specific detection methods using dyes or fluorescent dyes.[15,31−32] Recently, the application of IR spectroscopy using attenuated total reflection devices (ATR-FTIR spectroscopy) was reported.[33]

FTIR analysis is in principle a very useful method for the analysis of gases, since it is quick and allows a species-specific analysis, that is, not only activity but also selectivity information can be obtained. In its conventional form, however, only one channel is available, which means that FTIR spectroscopy can only be used as a sequential method. It was thus a major breakthrough when array detectors became available which could be used for FTIR imaging. This eliminates the need for the classical time-consuming step-and-collect mapping procedure for the acquisition of spatially resolved IR spectra.[9,21,24,34−35] FTIR imaging systems result from the combination of an infrared spectrometer, typically used in step-scan mode, and a focal plane array (FPA) detector.[26,34−37] The arrays used for the analysis contain several thousand elements on an area of only a few square millimeters, and each of the pixels can record a full IR spectrum. Recording the spectra takes typically only a few minutes, and using the rapid scan technique developed by Lauterbach and co-workers, this collection time can be decreased even further, making it possible to analyze transient processes.[35]

Previously used setups for the parallel analysis of catalyst performance based on FPA-FTIR spectroscopy used this technique in transmission mode; i.e., the gases leaving the reactor were guided into parallel gas cuvettes, which were imaged by the detection system, thus allowing simultaneous determination of the gas composition in the cuvettes.[9,12,21,26,34] However, the possible degree of parallelization is limited, since the connection of the reactor outlet to the parallel gas cuvette poses a major plumbing problem. Thus, in both setups described in the literature,[12,26] only 16-fold reactors

* To whom correspondence should be addressed. Phone: +49 (0) 208 306 2372. Fax: +49 (0) 208 306 2995. E-mail address: schueth@mpi-muelheim.mpg.de.

10.1021/cc049957e CCC: $27.50
Published on Web 03/30/2004

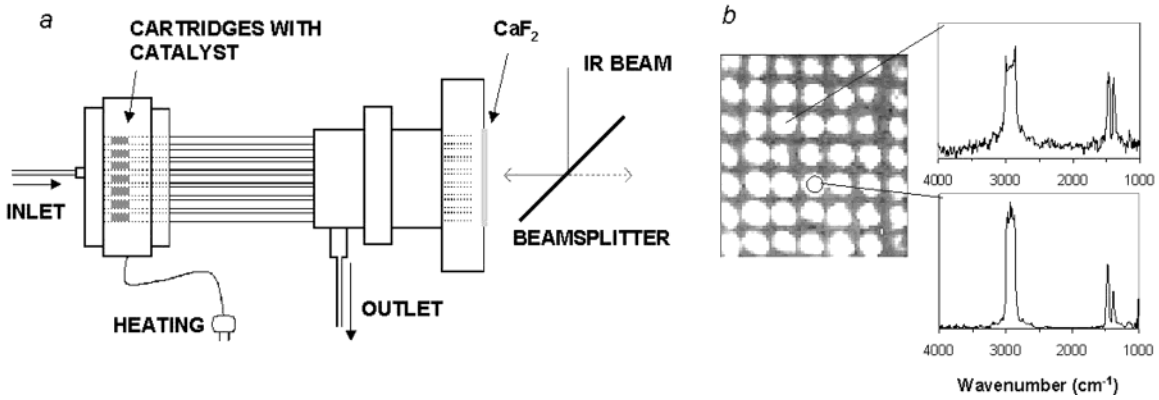

Figure 1. (a) Schematic view of the 49-fold reactor and the analysis cell for IR measurement in reflection mode. The reactor consists of a 7 × 7 capillary bundle; the stainless steel capillary inner diameter is ∼4 mm. Heating is provided by electrical cartridges. The IR beam is passed via a beam splitter (semitransparent mirror) into the reactor, passes through the gas phase, and is reflected back to the beam splitter by the gold-plated nozzles (b) View into the 7 × 7 capillary bundle, as followed on-line by FPA detector. The IR intensity is integrated in the 1000−8000 cm^{-1} range. Right top, IR spectrum of one pixel; right bottom, IR spectrum combined from ∼30 pixels.

have been used. The goal of this work was to circumvent this problem by using a reflection system, which is directly attached to the reactor and thus allows a much higher degree of parallelization. As a model reaction, pentane hydroisomerization was chosen. This is on one hand a relatively simple reaction with little byproduct formation with most catalysts, on the other hand, it is a very demanding reaction with respect to IR-product analysis, since the spectra of pentane and isopentane do not differ much. For evaluation of the method, it is thus ideally suited, since if the products from this reaction can be reliably analyzed, other reactions should be much easier to investigate with the system described. In addition, the reaction is of high relevance in the petroleum industry, and a high degree of sophistication has already been achieved for that reaction in conventional systems,[38−43] so that benchmarking is easy.

Experimental Section

A schematic view of the reactor and the analysis cell is given in Figure 1. The reactor consists of a capillary bundle in square 7 × 7 arrangement. The length of the bundle is ∼20 cm, and the capillary inner diameter is 4 mm. Each capillary is at the inlet end of the analysis cell equipped with a gold-coated nozzle with a 0.5-mm-diameter channel for gas inlet. The heating is provided by three electrical heating cartridges incorporated into the stainless heating part. The temperature in the heating part is controlled by a thermocouple placed close to the heating element.

To avoid contamination of the reactor and to make loading of the reactor easier, the catalyst is placed in 10-mm-long stainless steel cartridges (4-mm i.d.), which are inserted into the bores in the heated part. A sinter metal frit in the bottom of each cartridge supports the catalyst, which can be used as powder or split. In our experiments, we used the fraction between 250 and 500 μm.

Gaseous reaction mixture is fed into the reactor through one common inlet connected to the removable top of the reactor. The gas inlet system consists of a liquid/gas mixer, where carrier gas (H_2) is mixed with liquid *n*-pentane and then introduced into the reactor. The H_2 and *n*-pentane flow is controlled by mass flow controllers (Bronkhorst). Concentration of *n*-pentane in the reaction mixture was typically 2.5 vol %; linear flow through the reactor was 157.5 mL/min, that is, 3.2 mL/min per channel; and total pressure, 1 bar.

The product gas stream from each catalyst is directly fed into the analysis capillaries through the nozzles so that no additional connections have to be made. The outlet of all capillaries is mixed together at the end of the analysis channels and vented. The end of the capillary bundle is fitted with an infrared transparent CaF_2 window (Figure 1a). This window is placed in ∼1 mm distance from the capillary outlets, leaving only a relatively small space for mixing of the gases coming out of the capillaries. Products of the catalytic reaction are analyzed simultaneously by reflection IR spectroscopy with detection by FPA detector. Since the optical path through the mixed gas is only ∼1 mm long, as compared to the 200-mm length of the capillaries, errors due to mixing of the gas are sufficiently small to be neglected.

We have, together with Bruker, developed an imaging optics which allows the use of the external port of a step-scan FTIR spectrometer to pass the IR beam through a 4 × 4-cm gas cell and direct it to a FPA detector. The optical setup used in this study thus consists of a step-scan FTIR spectrometer, a system of gold-coated mirrors, a beam splitter, and a mercury cadmium telluride (MCT) FPA detector. The FPA detector consists of a large number of very small infrared detectors arranged in a rectangular grid pattern.[21,24,36,44] When incorporated into an imaging system, radiation from different areas of the sample falls on different areas of the detector, allowing both spatial and spectral information to be collected simultaneously. The FPA and the FTIR spectrometer are connected such that the modulation of the IR source by the interferometer is synchronized with the collection by the FPA. In operation, a series of images is collected as a function of interferometer optical path difference. After Fourier transformation of the modulated signal, IR spectra are obtained for every spatial location in the image plane. The spectral resolution is determined by the optical retardation of the interferomete, and the spatial resolution depends on the optical configuration and wavelength.

An FTIR spectrometer (Equinox 55, Bruker) was used as a IR light source; the IR light beam passes through a system of gold-mirrors and is focused onto a semitransparent beam splitter (Figure 1a). Part of the IR radiation is transmitted into the capillaries of the capillary bundle and reflected by the gold-coated mirror at the end of each capillary. This reflected part of the IR beam contains the information on the composition of the gas phase in each reactor capillary. The combined light beams behind the beam splitter pass through the system of gold mirrors and are focused onto the 64 × 64-pixel mercury cadmium telluride (MCT) FPA detector operated at liquid nitrogen temperature.

This system is capable to collect a spectral imaging data set consisting of 64 × 64 spatially resolved pixels (4096 spectra) in the 1000−8000 cm^{-1} spectral range with 8 cm^{-1} spectral resolution in ∼10 min. The field of view is ∼4 × 4 cm, which covers the footprint size of the reactor 7 × 7 square capillary bundle. The resolution of 64 × 64 pixesl in the 4 × 4-cm analysis plane corresponds to a point-to-point resolution of ∼0.62 mm.

Commercial γ-Al_2O_3 (D 10-10; BASF) and commercial Pt-mordenite (0.4% Pt, Hysopar SN 058 H/00; Südchemie) were used as benchmarks for commissioning of the system. A set of new catalysts (1% Pt) was prepared by incipient wetness impregnation of NH_4-MOR (CRV 10A; Zeolyst) with Pt salt ($Pt(NH_3)_4(NO_3)_2$; ABCR) and subsequent calcination at different temperatures. This procedure led to the formation of catalysts with different activities in *n*-pentane hydroisomerization. For the catalytic test, 30 mg of catalyst was mixed with 70 mg of inert Al_2O_3 and placed into each cartridge. Prior to each experiment, the catalysts were activated in a stream of H_2 at 230 °C for 2 h.

For data processing and manipulation, in-house developed procedures and commercial software were used (e.g., Peak Fitting Module of Microcal Origin). The IR spectra of both *n*-pentane and isopentane (reactant and major product) show characteristic bands at 2900−3000 cm^{-1} (C−H stretching) and two bands in the 1300−1500 cm^{-1} (C−H bending) region. The IR spectra of both compounds are only slightly different, which makes the quantitative analysis problematic. However, it was found to be possible to use the difference in the spectral region of CH_3 symmetric scissors deformation (bands at 1385 and 1470 cm^{-1}) for quantitative analysis. The ratio of the band areas (1385 cm^{-1} vs 1470 cm^{-1}) in the IR spectra of pure *n*-pentane is ∼0.3, whereas in the spectra of pure isopentane, it is ∼0.7. The IR spectra of mixtures of *n*- and isopentane thus exhibit ratios of 1385 vs 1470 cm^{-1} band areas in the range 0.3−0.7, depending on the relative concentration of each compound. A calibration curve based on different peak area ratios for mixtures of known *n*-pentane and isopentane composition in the relative concentration range 0−100% was, therefore, used for quantitative analysis.

The main limit with respect to accuracy of this calibration is posed by the high demands on spectra quality. Light scattering, the effect of which is amplified due to the relatively complicated optical system and the long beam pathway, is the main reason for low signal-to-noise ratio in some cases. Although each pixel in the 64 × 64-pixel system contains a full IR spectrum, the signal-to-noise ratio in resulting spectra can substantially be improved by grouping the individual spectra from all pixels belonging to one channel, that is, ∼30−35 pixels (Figure 1b).

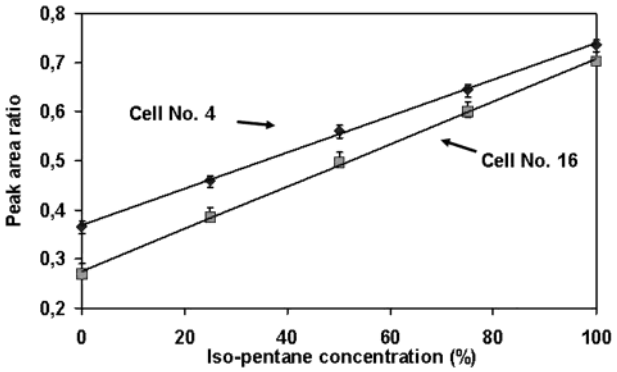

Figure 2. Calibration curves for determination of isopentane concentration in the mixtures of *n*-pentane and isopentane. The most extreme calibration curves (cells nos. 4 and 16) are depicted.

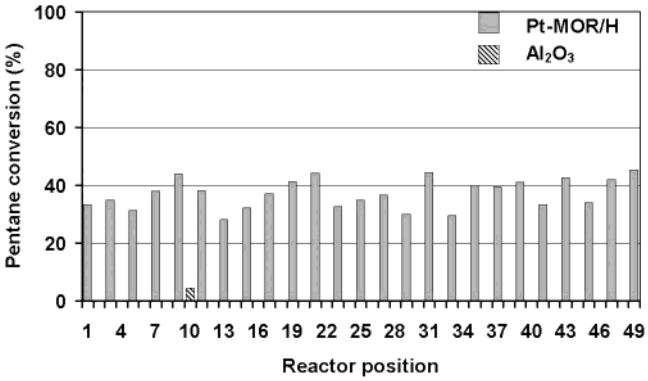

Figure 3. Catalytic activity measured in the reactor filled with reference catalysts Al_2O_3 and Pt-MOR/H (Hysopar) in a chessboard arrangement (Test 1). Set reaction temperature was 250 °C, time on-stream was 60 min. Average conversion in cells with Pt-MOR/H was 37.2 ± 5.2%; relative error was ±13.9%. Average conversion in cells with Al_2O_3 was 0.2%.

Results

Calibration. A set of measurements was performed with empty reactor and calibration mixtures containing *n*-pentane and isopentane in different concentrations. The spectra obtained for each individual reactor cell and different compositions (0, 25, 50, 75, and 100% of isopentane) of calibration mixture were processed using peak fitting and band area integration. Ideally, the linear calibration curves for all 49 cells should be identical because of the identical nominal path lengths and concentrations. In reality, however, differences were observed in the calibration curves for the different cells. These deviations can be traced back to different scattering and to deviations from perfect orthogonality of the mirrors with respect to the IR beam. This leads to effectively different beam paths. Figure 2 shows the two most extreme linear calibration curves. Therefore, for each cell a different calibration curve was used for further experiments.

Catalytic Tests. Several tests with different catalysts and catalyst arrangements were performed in order to examine the sensitivity of the system with respect to resolution between catalysts of different activity. Figure 3 shows results of a catalytic test that was performed with 24 reactor

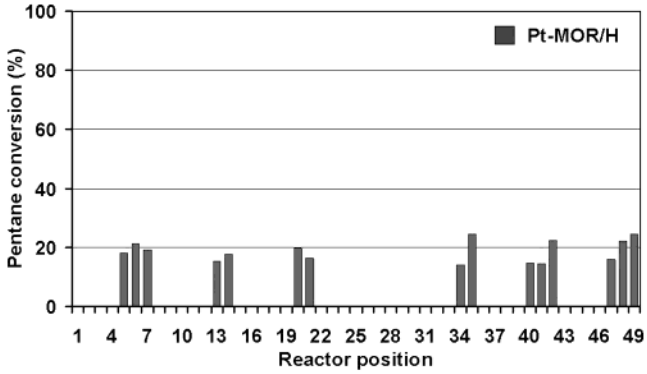

Figure 4. Catalytic activity measured in the reactor randomly filled with Al_2O_3, Pt-MOR/H (Hysopar) and Pt-MOR/300/0.3 (test 2). Set reaction temperature was 230 °C, time on-stream was 60 min. Average conversion in cells with Pt-MOR/H was 18.4 ± 3.7%; relative error was ±19.9%. Average conversion in cells with Al_2O_3 was 0.1%; in cells with Pt-MOR/300/0.3, 0%.

positions filled with Al_2O_3 (blank cells) and 25 positions filled with reference Pt-MOR/H (Hysopar) in a chessboard arrangement. As can be seen from Figure 3, the discrimination between the activity of the reference catalyst and blank cells is very good. The average *n*-pentane conversion under these conditions (250 °C; 2.5 vol % pentane) is ~37%, and the conversion detected in individual cells with reference Pt-MOR/H is in the range of 28.1−45.3%, which corresponds to a standard deviation of ±5.2%. The relative error can then be calculated to ±13.9%. Channels filled with Al_2O_3 did not display any activity, in agreement with expectations. In cell no. 10 with Al_2O_3, *n*-pentane was apparently isomerized to a small extent. However, the spectral quality for this particular cell was very bad so that the data calculated from this cell are very noisy.

Figure 4 describes results obtained in another test performed with the reactor randomly filled with blank (19× Al_2O_3), reference (15× Pt-MOR/H), and new catalysts of unknown activity (15× Pt-MOR/300/0.3). The reference Pt-MOR/H zeolite was identified as the only active catalyst, whereas the new Pt-MOR/300/0.3, as well as the blank samples, displayed no activity under these conditions (230 °C; 2.5 vol % pentane). The average conversion over the reference catalyst under these conditions was 18.4 ± 3.7%; the detected conversion in individual cells with reference catalyst was in the range of 14.1−24.6%. The corresponding relative error was ±19.9%.

To provide further information on the range of the catalytic data reliability, the system was used for testing 10 different Pt-MOR catalysts pretreated under various conditions and, thus, exhibiting different activity in *n*-pentane isomerization. The results of these experiments are described in Figure 5 and Table 1. The data show that one can easily distinguish between catalysts of different activity. The standard deviation between cells corresponding to identical catalysts is always below ±20% rel. The most active catalyst (reference Pt-MOR/H, no. 8) under these conditions (300 °C, 2.5% pentane) had an average conversion of 76.2% (close to the thermodynamic equilibrium), and the activity in each individual cell with this catalyst was in the range of 72−81%, giving a standard deviation of ±3.6% and corresponding relative error of ±4.7%. Similar results with a relative error

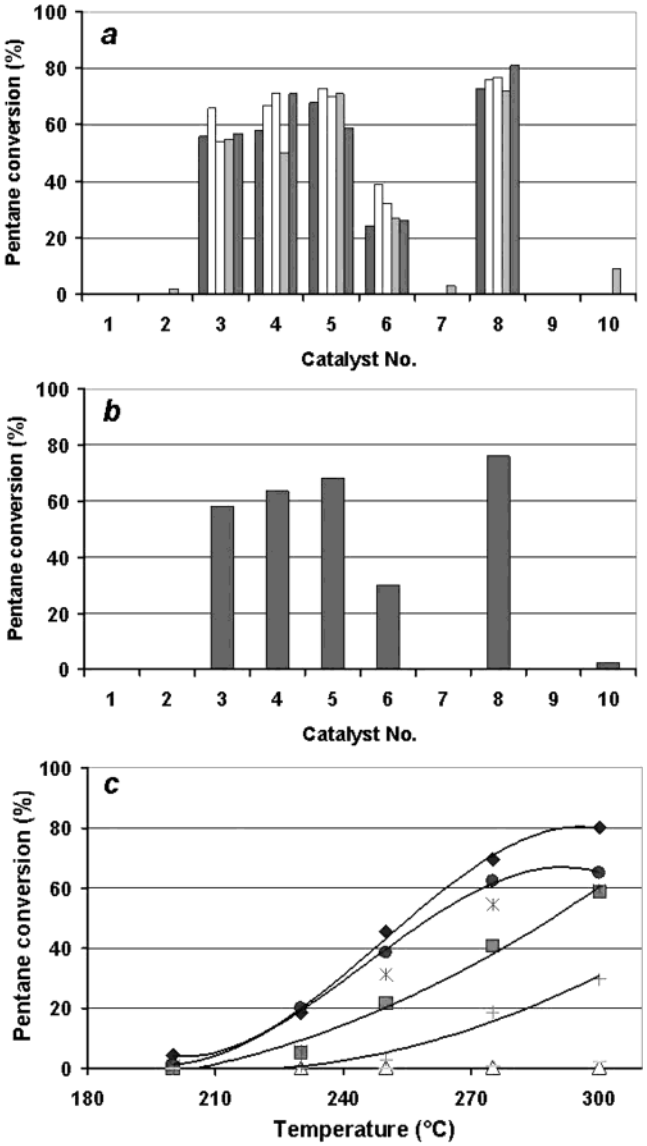

Figure 5. Catalytic activity measured in reactor randomly filled with Al_2O_3 and 9 different Pt-MOR catalysts (test 3). Set reaction temperature was 300 °C, time on-stream was 60 min. Description of catalysts nos. 1−10 is given in Table 1. (a) The catalytic activities as measured in individual cells with identical catalysts are plotted as a group together. Relative error between cells with the same catalyst did not exceed ±20% rel and was typically appreciably lower. (b) The catalytic activity averaged through all cells filled with the same catalyst. (c) Averaged activity of the 10 different catalysts measured at different set reaction temperatures: (♦) Pt-MOR/H, (△) Pt-MOR/300, (■) Pt-MOR/400, (*) Pt-MOR/500, (●) Pt-MOR/600, (+) Pt-MOR/700, (−) Pt-MOR/800, and (−) Pt-MOR/300/0.3. Catalysts nos. 1 and 9 displayed no catalytic activity.

of at most 20% were obtained for cells with catalysts nos. 3−6 (see Figure 5a and Table 1).

The averaged data on the catalyst activity for each set of five identical catalysts obtained in that experiment (10 different Pt-MORs) are depicted in Figure 5b. The averaged catalytic activity of these catalysts at different temperatures is shown in Figure 5c. Clear trends for each group of catalysts can be identified, and the observed activity trends for these catalysts have a reasonable explanation with respect to their way of preparation and activation, such as different acidity, Pt distribution, etc. (see below). The same activity trends have been observed on some of these Pt-MOR catalysts by

Table 1. Summarized Data of the Catalyst Activity, as Measured in the 49-Cell Reflection Setup[a]

catalogue no.	catalyst	total, cells	av X,[b] %	min X,[c] %	max X,[d] %	SD,[e] %	rel error,[f] %
test 1, $T = 250$ °C							
1	Al_2O_3[g]	24	0.2	0.0	4.4		
2	Pt-MOR/H	25	37.2	28.1	45.3	5.2	13.9
test 2, $T = 230$ °C							
1	Al_2O_3	19	0.1	0.0	4.6		
2	Pt-MOR/300/0.3	15	0,0	0.0	0.0		
3	Pt-MOR/H	15	18.4	14.1	24.6	3.7	19.9
test 3, $T = 300$ °C							
1	Pt-MOR/UN[h]	5	0.0	0.0	0.0		
2	Pt-MOR/300[i]	5	0.4	0.0	2.0		
3	Pt-MOR/400[i]	5	58.1	54,0	66.0	4.8	8.3
4	Pt-MOR/500[i]	5	63.8	50.0	71.0	9.1	14.4
5	Pt-MOR/600[i]	5	68.5	59.0	73.0	5,4	8
6	Pt-MOR/700[i]	5	29.9	24.0	39.0	6.0	20.1
7	Pt-MOR/800[i]	5	0.6	0.0	3.0		
8	Pt-MOR/H	5	76.2	72.0	81.0	3.6	4.7
9	Al_2O_3	5	0.0	0.0	0.0		
10	Pt-MOR/300/0.3[j]	4	2.4	0.0	9.0		

[a] Time on-stream, 60 min. [b] Average conversion. [c] Minimal detected conversion in coherent cells. [d] Maximal detected conversion in coherent cells. [e] Standard deviation between individual coherent cells. [f] Relative error of data from all coherent cells. [g] Pt-MOR/H: Hysopar SN058 H/00, Südchemie; reference catalyst. [h] Pt-MOR/UN: Pt-MOR prepared by Pt impregnation of NH_4-MOR (CRV 10A, Zeolyst); uncalcined. [i] Pt-MOR/300−800: Pt-MOR prepared by Pt-impregnation of NH_4-MOR calcined at 300−800 °C, fast temperature increase during calcination (2 °C/min). [j] Pt-MOR/300/0.3: Pt-MOR prepared by Pt impregnation of NH_4-MOR, calcined at 300 °C, slow temperature increase during calcination (0.3 °C/min).

catalytic tests in a conventional catalytic setup in the group of J. Lercher at TU München. Direct comparison of observed rates is difficult, though, since the conventional setup is designed for different reaction parameters, such as pressure and flow rates.

Discussion

The data presented show that the system described here is suitable for highly parallelized analysis of catalyst activity, whereas not only activity information but also selectivity information is accessible due to the species-specific analysis with IR spectroscopy. For the case study of *n*-pentane hydroisomerization, the relative error of ±20% rel is rather large, and the system is, thus, more suitable for prescreening, where such an error is more than acceptable. However, for more fortunate cases with IR spectra that can be differentiated more easily, precise analysis with the system will be possible.

The observed deviations for identical catalysts are due to several factors: The main contribution is light scattering, which has a negative effect on the spectra quality and, thus, on the exact determination of peak area. This problem is made even more severe because the decisive peaks are strongly overlapping. There is also some error in the calibration, because the dependence of peak ratio on the isopentane concentration is very flat. To ensure the highest possible accuracy of the calibration, 49 individual equations, one for each reactor cell, are used.

Another contribution results from the temperature inhomogeneity over the reactor, created by the thermal profile around the heating elements. The measured temperature in the individual reactor positions varied from 218 °C (corner positions close to the heating cartridges) to ∼204 °C (middle positions) at a set temperature of 230 °C. This contribution is relatively low in comparison to the errors brought about by light scattering and can be neglected if the system is used for prescreening. Full or partial elimination of the errors due to thermal inhomogeneity is possible by different means: (i) one could use a different heating system which produces lower gradients, such as encapsulating the whole reactor in an oven; or (ii) one could calibrate the temperatures by recording for each individual channel the deviation between set point and real temperature for empty channels, assuming that this difference would be similar under reaction conditions. It is clearly advantageous, however, to fully eliminate the gradients by a different design of the heating, as has been shown to be possible to a large extent for other reactors described by us.[8,12,16−18]

With respect to the catalytic activity of the differently pretreated samples, the differences are easily explained in terms of the history of the samples. If the catalysts are not treated at sufficiently high temperatures, two different factors are not optimized: (i) high-temperature treatment leads to autoreduction of the platinum, providing the hydrogenation/dehydrogenation activity necessary for a bifunctional isomerization catalyst. A temperature of 300 °C may not be sufficient for full reduction of the platinum. (ii) To create the acid sites, the ammonium form of the catalyst has to be converted to the H form. Also for this, sufficiently high temperatures are necessary. In a temperature range for the pretreatment between 400 and 600 °C, catalyst performance is satisfactory, with the optimum apparently lying between 500 and 600 °C. After pretreatment at higher temperature, the noble metal particles start to sinter, and the zeolitic framework is destroyed.[45−47] This explains the low activity of the samples pretreated at 700 and 800 °C. Pt sintering after pretreatment at higher temperatures has also been observed for our samples using TEM in the group of R. Schlögl at FHI Berlin.

Conclusion and Outlook

Reflection FPA-FTIR spectroscopy is introduced as a viable method to analyze activity and selectivity of catalyst

libraries with a relatively high degree of parallelization. The described 49-cell reactor with FPA-IR optical setup is able to provide at least semiquantitative information about the activity of different catalysts with a throughput of 49 catalysts/day if a full temperature/activity curve is recorded. The relative error of the analysis was at most 20% rel, in most cases below 10% rel.

The system may even be more useful for the investigation of other gas-phase reactions, in which the discrimination between IR spectra of reactant and product is not as difficult. For such reactions, the system can probably be used in a fully quantitative mode, which would make it faster than any other hitherto described system operating in a close-to-conventional mode. DeNOx reactions are such a class of reactions in which the analysis should be substantially more straightforward and precise.

In principle, also, the degree of parallelization can be increased, with the theoretical limit given by the size of one pixel. However, scattering problems will increase for more highly parallelized systems, and thus, the full theoretical limit can most probably not be achieved.

Acknowledgment. This study was supported by the German Federal Ministry of Education and Science (BMBF) under project number 03C0307A. We would also like to thank Ch. Woltz from J. Lercher's group and F. Jentoft from R. Schlögl's group, who provided some unpublished data for comparison.

References and Notes

(1) Thomas, R.; Moulijn, J. A.; De Beer, V. H. J.; Medema, J. *J. Mol. Catal.* **1980**, *8*, 161.
(2) Creer, J. G.; Jackson, P.; Pandy, G.; Percival, G. G.; Seddon, D. *Appl. Catal*. **1986**, *22*, 85.
(3) Moates, F. C.; Somani, M.; Annamalai, J.; Richardson, J. T.; Luss, D.; Wilson, R. C. *Ind. Eng. Chem. Res*. **1996**, *35*, 4801.
(4) Senkan, S. *Nature* **1998**, *394*, 350.
(5) Holzwarth, A.; Schmidt, H.-W.; Maier, F. *Angew. Chem., Int. Ed. Engl*. **1998**, *37*, 2644.
(6) Jandeleit, B.; Turner, H. W.; Uno, T.; Van Beek, J. A. M.; Weinberg, W. H. *CATTECH*, **1998**, *2*, 101.
(7) Cong, P.; Doolen, R. D.; Fan, Q.; Giaquinta, D. M.; Guan, S.; McFarland, E. W.; Pooraj, D. M.; Self, K.; Turner, H. W.; Weinberg, W. H. *Angew. Chem., Int. Ed. Engl*. **1999**, *38*, 484.
(8) Hoffmann, C.; Wolf, A.; Schüth, F. *Angew. Chem., Int. Ed. Engl.* **1999**, *38*, 2800.
(9) Snively, C. M.; Katzenberger, S.; Oskarsdottir, G.; Lauterbach, J. *Opt. Lett.* **1999**, *24*, 1841.
(10) Newsam, J. M.; Schüth, F. *Biotechnol. Bioeng.* **1999**, *61*, 203.
(11) Senkan, S. *Angew. Chem*. **2001**, *113*, 322.
(12) Schüth, F.; Busch, O.; Hoffmann, C.; Johann, T.; Kiener, C.; Demuth, D.; Klein, J.; Schunk, S.; Strehlau, W.; Zech, T. *To. Catal*. **2002**, *21*, 55.
(13) Jandeleit, B.; Schaefer, D. J.; Powers, T. S.; Turner, H. W.; Weinberg, W. H. *Angew. Chem., Int. Ed. Engl.* **1999**, *38*, 2495.
(14) Claus, P.; Hönicke, D.; Zech, T. *Catal. Today* **2001**, *67*, 319.
(15) Busch, O. M.; Hoffmann, C.; Johann, T. R. F.; Schmidt, H.-W.; Strehlau, W.; Schüth, F. *J. Am. Chem. Soc*. **2002**, *124*, 13527.
(16) Kiener, C.; Kurtz, M.; Wilmer, H.; Hoffmann, C.; Schmidt, H.-W.; Grunwaldt, J.-D.; Muhler, M.; Schüth, F. *J. Catal.* **2003**, *216*, 110.
(17) Hoffmann, C.; Schmidt, H. W.; Schüth, F. *J. Catal*. **2001**, *198*, 348.
(18) Thompson, S.; Hoffmann, C.; Ruthe, S.; Schmidt, H.-W.; Schüth, F. *Appl. Catal., A* **2001**, *220*, 253.
(19) Senkan, S.; Ozturk, S. *Angew. Chem., Int. Ed. Engl*. **1999**, *38*, 791.
(20) Orschel, M.; Klein, J.; Schmidt, H.-W.; Maier, W. F. *Angew. Chem., Int. Ed. Engl*. **1999**, *38*, 2791.
(21) Snively, C. M.; Oskarsdottir, G.; Lauterbach, J. *Catal. Today* **2001**, *67*, 357.
(22) Kibbey, C. E. In *A Practical Guide to Combinatorial Chemistry*; Czarnik, A. W., DeWitt, S. H., Eds.; American Chemical Society: Washington, DC, 1997, p 199.
(23) Wilkin, O. M.; Maitlis, P. M.; Haynes, A.; Turner, M. L. *Catal. Today* **2003**, *81*, 309.
(24) Snively, C. M.; Oskarsdottir, G.; Lauterbach, J. *J. Comb. Chem.* **2000**, *2*, 243.
(25) Haap, W. J.; Walk, T. B.; Jung, G. *Angew. Chem., Int. Ed. Engl*. **1998**, *37*, 3311.
(26) Snively, C. M.; Oskarsdottir, G.; Lauterbach, J. *Angew. Chem., Int. Ed. Engl*. **2001**, *40*, 3028.
(27) Taylor, S.; Morken, J. *Science* **1998**, *280*, 267.
(28) Reetz, M. T.; Becker, H. H.; Kühling, K. M.; Holzwarth, A. *Angew. Chem., Int. Ed. Engl*. **1998**, *37*, 2647.
(29) Johann, T.; Brenner, A.; Schwickardi, M.; Busch, O.; Marlow, F.; Schunk, S.; Schüth, F. *Angew. Chem., Int. Ed. Engl.* **2002**, *41*, 2996.
(30) Johann, T.; Brenner, A.; Schwickardi, M.; Busch, O.; Marlow, F.; Schunk, S.; Schüth, F. *Catal. Today* **2003**, *81*, 449.
(31) Reddington, E.; Sapienza, A.; Guraou, B.; Viswanathan, R.; Sarangapani, S.; Smotkin, E. S.; Mallouk, T. E. *Science* **1998**, *280*, 1735.
(32) Schüth, F.; Brenner, A.; Schunk, S. A.; Stichert, W.; Lange de Oliveira, A.; Unger, K. German Patent DE 19830607.5; July 7, 1999.
(33) Leugers, A.; Neithamer, D. R.; Sun, L. S.; Hetzner, J. E.; Hilty, S.; Hong, S.; Krause, M.; Bayerlein, K. *J. Comb. Chem.* **2003**, *5*, 238.
(34) Snively, C. M.; Lauterbach, J. *Spectroscopy* **2002**, *17*, 26.
(35) Hendershot, R. J.; Fanson, P. T.; Snively, C. M.; Lauterbach, J. A. *Angew. Chem., Int. Ed. Engl.* **2003**, *42*, 1152.
(36) Lewis, E. N.; Treado, P. J.; Reeder, R. G.; Story, G. M.; Dowrey, A. E.; Marcott, C.; Levin, I. W. *Anal. Chem*. **1995**, *67*, 3377.
(37) Lewis, E. N.; Levin, I. W. *Appl. Spectrosc*. **1995**, *49*, 672.
(38) Hollo, A.; Hancsok, J.; Kallo, D. *Appl. Catal., A* **2002**, *229*, 93.
(39) Miyaji, A.; Echizen, T.; Li, L.; Suzuki, T.; Yoshinaga, Y.; Okuhara, T. *Catal. Today* **2002**, *74*, 291.
(40) Ivanov, A. V.; Vasina, T. V.; Masloboishchikova, O. V.; Khelkovskaya-Sergeeva, E. G.; Kustov, L. M.; Houzvicka, J. I. *Catal. Today* **2002**, *73*, 95.
(41) Rossi, S.; Ferraris, G.; Valigi, M.; Gazzoli, D. *Appl. Catal., A* **2002**, *231*, 173.
(42) Chica, A.; Corma, A.; Miguel, P. J. *Catal. Today* **2001**, *65*, 101.
(43) Yamaguchi, T. *Appl. Catal., A* **2001**, *222*, 237.
(44) Treado, P. J.; Levin, I. W.; Lewis, E. N. *Appl. Spectrosc*. **1994**, *48*, 3311.
(45) Zheng, J.; Dong, J. L.; Xu, Q. *Stud. Surf. Sci. Catal.* **1994**, *84*, 1641.
(46) Creyghton, E. J.; Van Duin, A. C. T.; Jansen, J. C.; Kooyman, P. J.; Zandbergen, H. W.; VanBekkum, H. *J. Chem. Soc., Faraday Trans.* **1996**, *92*, 4637.
(47) Khodakov, A.; Barbouth, N.; Oudar, J.; Villain, F.; Bazin, D.; Dexpert, H.; Schulz, P. *J. Phys. Chem. B* **1997**, *101*, 766.

CC049957E